J. Kor. Soc. Fish. Tech., 47 (1), 046 – 058, 2011
DOI:10.3796/KSFT.2011.47.2.046

FISHERIES TECHNOLOGY
www.fishtech.or.kr

The study of simplified technique compared with analytical solution method for calculating the energy consumption loads of four houses having various wall construction

Kyu-Il HAN*

Department of Mechanical System Engineering, Pukyong National University, Busan 608-739, Korea

A steady-state analysis and a simple dynamic model as simplified methods are developed, and results of energy consumption loads are compared with results obtained using computer to evaluate the analytical solution. Before obtaining simplified model a mathematical model is formulated for the effect of wall mass on the thermal performance of four different houses having various wall construction. This analytical study was motivated by the experimental work of Burch et al. An analytical solution of one-dimensional, linear, partial differential equation for wall temperature profiles and room air temperatures is obtained using the Laplace transform method. Typical Meteorological Year data are processed to yield hourly average monthly values. This study is conducted using weather data from four different locations in the United States: Albuquerque, New mexico; Miami, Florida; Santa Maria, California; and Washington D.C. for both winter and summer conditions. The steady state analysis that does not include the effect of thermal mass can provide an accurate estimate of energy consumption in most cases except for houses #2 and #4 in mild weather areas. This result shows that there is an effect of mass on the thermal performance of heavily constructed house in mild weather conditions. The simple dynamic model is applicable for high cycling rates and accurate values of inside wall temperature and ambient air temperature.

Keywords: Steady state, Energy consumption load, Thermal mass, One-dimensional, Thermal performance

Introduction

A great deal of work has been done and many methods have been developed to obtain energy consumption loads for buildings. Some works (Mitalas et al., 1967, 1968) use the transfer function approach for calculating energy loads. This concept is first introduced by them using what they call room thermal response factors (Stephenson et al., 1967).

Their procedure is as follows: the room surface temperatures and cooling or heating load are first calculated in a rigorous manner for several typical constructions. In these calculations, the components such as solar heat gain, conduction heat gain, or heat gain from lighting, equipment, and occupants are

*Corresponding author: kihan@pknu.ac.kr, Tel: 82-51-629-6194, Fax: 82-51-629-6188

simulated by pulses of unit strength. The transfer functions are then calculated as numerical constants which represent the cooling or heating load excitation pulses corresponding to the input excitation pulses.

The method of Mitalas (1968) assumes that heat flow through building elements is one-dimensional, i.e. effects of room corners or other irregularities are ignored, and that room air temperature is uniform throughout the room. This method can handle periodic or non-periodic ambient conditions and variable surface heat transfer coefficients.

Peavy et al. (1973) and Kusuda (1976) also use a response factor method for their computer program to calculate building loads. It is concluded that a combination of mass in walls and roof facing the interior with insulation placed on the outer surfaces of a building is very effective in reducing and controlling the variation of the indoor air temperature. Kusuda conducts a computer program for prediction of dynamic thermal and energy loads of buildings is presented. Those results are compared with experimental results obtained from laboratory measurements made on an experimental building.

Kusuda (1981) compares computer simulation results with the method developed by ASHRAE' s Technical Committee on energy calculation. However, transient effects brought about through controls (time dependent thermostat and fan switch setting) are not included, and thermal storage effects of the building components and dead-band control also are not simulated.

A finite differences method is used by Cuplinskas (1977) for thermal response calculations. The finite differences method is frequently used to solve more complex dynamic problems in heat transfer than can be handled by analytical methods. His proposed method is not meant as a substitute for the more elaborate methods, but as an alternative simplified solution that is easily understood and programmed by engineers.

A degree-day method is used by Webster (1985) for small buildings. The method is based on the principle that the energy requirement for space heating is primarily dependent on the difference in temperature between indoors and outdoors.

In Jones et al. (1982), an evaluation is made of the thermal performance of 4 double-envelope house built in Middletown, Rhode Island. It is concluded that the low heating energy needs of the house are due primarily to the excellent insulative value of the double shell. The double-shell construction of the house results in very low air infiltration, even on windy days.

Similar results for investigating which construction materials consume less energy under varying climatic conditions are obtained by Burch et al. (1984). His group recently conducted experiments on six test buildings in Gaithersburg, MO. These buildings were instrumented to measure heating and cooling loads, and indoor comfort. They focus on the effect of different construction materials in determining the energy consumption load.

All of these studies are deficient in one or more ways. The experimental studies exhibit a very small savings due to mass of the same magnitude as the effect of solar radiation absorbed by and transmitted through the walls. The analytical studies do not include a realistic model of the energy plant.

The main purpose of this study is to develop a simplified method from a rigorous mathematical basis to analyze the energy consumption load and calculating the cycling time corresponding to on-off controller and to compare the results with the

analytical solution.

Theoretical formulation for analytical solution

The formulation of an analytical method for obtaining wall temperature profile, room air temperature, and energy consumption load is presented. Four of the six houses studied by Burch et al. are modelled. Each test house is a 6.1m by 6.1m by 2.3m one-room house. The houses have identical floor plans and orientations, and are identical except for wall construction, which is as follows: insulated lightweight wood frame; insulated masonry with outside mass; uninsulated masonry; and insulated masonry with inside mass.

Table 1. Wall construction types

House #1 : insulated lightweight wood frame
13mm (0.5 in) gypsum board 0.05mm (0.002 in) polyethylene film 50 × 100 mm (2 × 4 in) studs placed 410 mm (16 in) o.c. with R-11 16 mm (5/8 in) exterior plywood
House #2 : insulated masonry (outside mass)
13mm (0.5 in) gypsum board 0.05mm (0.002 in) polyethylene film 51 mm (2 in) thick extruded polystyrene insulation placed between 38 mm (1 − 1/2 in) wide wood furring strips placed 610 mm (24 in) o.c. 6.4 mm (1/4 in) air space 100mm (4 in) 2-core hollow concrete block 1680 kg/m3 (105 lb/ft3) 100 mm (4 in) face brick
House #3 : uninsulated masonry
13mm (0.5 in) gypsum board 0.05mm (0.002 in) polyethylene film 20 mm (3/4 in) air space created by 50 × 20 mm (2 × 3/4 in) furring strips placed 410 mm (16 in) o.c. 200 mm (8 in) 2 − core hollow concrete block 1680 kg/m^3 (105 lb/ft3)
House #4 : insulated masonry (inside mass)
13 mm (0.5 in) plaster 200 mm (8 in) 2 − core hollow concrete block 1680 kg/m^3 (105 lb/ft3) 89mm (3 − 1/2 in) perlite insulation in space between block and brick 100 mm (4 in) face brick

The details of the wall construction for each of the four houses are presented in Table 1.

Weather data for four cities in the United States are used in this study. Twenty-four discrete data points calculated from TMY (Typical Meteorological Year) weather data files (1998) are converted to continuous form via a Fast Fourier Transform (Brigham, 2004). Each house is modelled by a single homogeneous wall and an air node.

The system is considered as one-dimensional. The heat transfers in the y and z directions are assumed to be negligible, and the heat flow occurs principally in the direction perpendicular to the surface of the wall (x-direction). Neglect of heat flow in the y and z directions should not significantly affect the applicability of the solution (Myers, 2001).

Under this study there is no heat generation within the wall, and the energy balance, after some manipulation, yields:

$$\partial^2 T/\partial x^2 = (1/\alpha)\partial T/\partial t \quad (1)$$

Two corresponding boundary conditions to the above linear, second-order, partial differential equation are:

$$-k\partial T/\partial x\ (x=0) = \hat{a}S^* + h_e\ (T_\infty - T_0) \quad (2)$$

$$-k\partial T/\partial x\ (x=L) = -h_i\ (T_A - T_L) \quad (3)$$

The initial condition for the wall temperature is expressed in polynomial form as:

$$T\ (x,\ 0) = \sum_{n=0}^{4} a_n x^n \quad (4)$$

The energy balance for the room air temperature including heat transfer from the inside surface of the wall, infiltration loss, and auxiliary heat input Q, is:

$$C_A dT_A/dt = -h_i A\ (T_A - T_L) - C_A' I\ (A_A - T_\infty) + Q \quad (5)$$

$$C_A=(\rho C_v)_A V_A \tag{6}$$

$$C_A'=(\rho C_p)_A V_A \tag{7}$$

$$I'=C_A' I/C_A \tag{8}$$

The parameters, h_i, h_e, C_A, C_A' and I are assumed constant.

The corresponding initial condition to equation (5) is as follows:

$$T_A(0)=T_i \tag{9}$$

Weather data for four cities in the United States are used in this study. Those cities under study are Albuquerque, NM; Miami, FL; Santa Maria, CA; and Washington, D.C. Two of the cities, Albuquerque and Washington D.C., have four distinct seasons, while Santa Maria experiences mild weather conditions year round. Miami weather is the hottest of the four cities studied, and houses need to be cooled nearly year round. TMY (Typical Meteorological Year) weather data files are used to obtain hourly values of the solar flux and ambient temperature.

The weather data input to the analytical model is finally represented in the following form:

$$S^*(t)=b_0+\sum_{i=1}^{11}[b_i\cos(w_i t+\Phi_i)+c_i\sin(w_i t+\Phi_i)] \tag{10}$$

$$T_\infty(t)=d_0+\sum_{i=1}^{11}[d_i\cos(w_i t+\Phi_i)+e_i\sin(w_i t+\Phi_i)] \tag{11}$$

where b_0 is the DC component of the solar flux and d_0 is the DC component of the ambient temperature.

The Laplace transform solution technique (Kreyszig, 2006) is successfully applied to the problem under study, and the inversion from the Laplace domain to the time domain is accomplished using the complex inversion theorem using Bromwich contour (Carslaw et al., 1959).

The form of the wall temperature as a function of time is:

$$\begin{aligned}T(x,t)=&\sum_{m=1}^{\infty}[(A_m/C_m)\mathrm{EXP}(-\alpha\eta_m^2 t)\cos(\eta_m x)\\&+(B_m/C_m)\mathrm{EXP}(-\alpha\eta_m^2 t)\sin(\eta_m x)]\\&+a_0+a_1x+a_2x^2+a_3x^3+a_4x^4+2\alpha a_2 t\\&+12\alpha^2 a_4 t^2+6\alpha a_3 xt+12\alpha a_4 x^2 t\\&+(1/2)[(N_1/D)(t^2+tx^2/\alpha+x^4/(12\alpha^2))\\&+(N_1'/D)(2t+x^2/\alpha)+N_1''/D-D''N_1/D^2\\&-(2D'/D^2)[(t+x^2/(2\alpha))N_1+N_1']\\&+2D'^2N_1/D^3+(N_2/D)(t^2x+tx^3/(3\alpha)\\&+x^5/(60\alpha^2))+(N_2'/\mathrm{D})(2tx+x^3/(3\alpha))\\&+N_2''x/D-D''N_2x/D^2-(2D'/D^2)[(tx\\&+x^3/(6\alpha))N_2+N_2'x]+2D'^2N_2x/D^3]\\&+\sum_{i=1}^{11}[x_{1i}(x)\cos(w_i t)+x_{2i}(x)\sin(w_i t)]\end{aligned} \tag{12}$$

The form of the room air temperature as a function of time is:

$$\begin{aligned}T_A(t)=&\sum_{m=1}^{\infty}[(A_m/C_m)\mathrm{Mcos}(\eta_m L)\ \mathrm{EXP}(-\alpha\eta_m^2 t)\\&+(B_m/D_m)\ \mathrm{Msin}(\eta_m L)\mathrm{EXP}(-\alpha\eta_m^2 t)\\&+((c_{32}+c_{36})/c_{33}-c_{39}+c_{42}+T_i)\ \mathrm{EXP}\\&(-\beta t)+(1/2)[F_6/F_1-(F_4D''+2F_5F_2)/(F_1)^2\\&+2F_4(F_2)^2+F_9/F_1-(F_7F_3+2F_8F_2)/(F_1)^2\\&+2F_7(F_2)^2/(F_1)^3]\\&+\sum_{i=1}^{11}[(x_{3i}+F_{10})\cos(w_i t)+(x_{4i}+F_{11})\sin(w_i t)]\\&+(Ma^*/\beta-Mc^*/\beta^2)t+Mc^*t^2/(2\beta)+c_{39}\end{aligned} \tag{13}$$

where η_m is the m^{th} root of the characteristic equation:

$$\tan(L\eta_m)=[-\eta_m(c_{14}s_m+c_{15})]/[c_{16}s_m^2+c_{17}s_m+c_{18}] \tag{14}$$

Attention is now turned to the process of switching modes, e.g. from heating to no heating. In the case of on-off control, this occurs when the room air temperature exceeds the dead band. This effects a partitioning in time, shown in Fig. 1, as

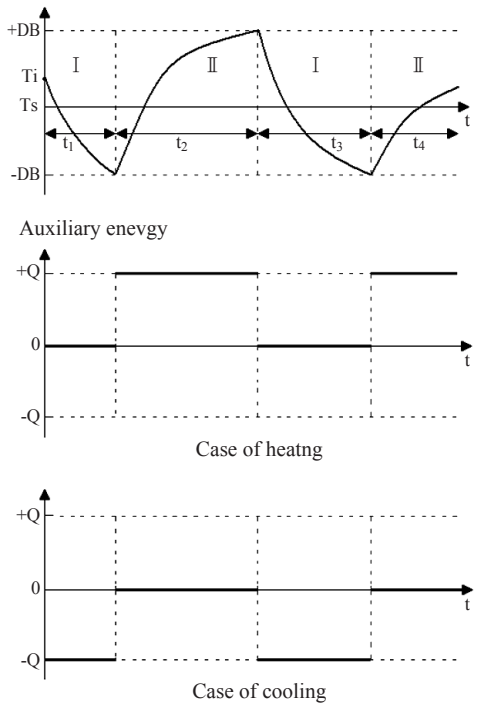

Fig. 1. Room air temperature trajectory and auxiliary energy input.

region I and region ll, when the heating system is "off" and "on", respectively.

Now we will discuss the steps used to obtain the times mentioned above for on-off control. We will illustrate the process during the heating season. First, the weather data, equations (10) and (11), are rearranged as follows:

$$S^* = b_0 + \sum_{i=1}^{11} [b_i \cos [w_i(t+t^*)] + c_i \sin[w_i(t+t^*)]] \tag{15}$$

$$T_\infty = d_0 + \sum_{i=1}^{11} [d_i \cos [w_i(t+t^*)] + e_i \sin[w_i(t+t^*)]] \tag{16}$$

where t^* is time at which the controller function changes.

In the first region:

1) Take initial conditions for the wall temperature, $T_w(x,t^*)$, and the room air temperature, T_i.
2) Let Q and t^* be zero. This arbitrarily implies no heating, and results in temperature decay as shown in Fig. 1.
3) Obtain t_1 using a bisection method.

In the second region:

1) Calculate a new initial condition by evaluating the solution for $T_w(x, t^*)$ and calculating coefficients a_0 to a_4 as presented in equation (4). The new initial state for $T_A = (-DB)$.
2) Let $Q = Q_{teating}$.
3) Take new weather data which is the original weather data shifted by $w_i t_1$ (i.e. $w_i t^*$).
4) Obtain t_2 using a bisection method.

The process repeats until a complete daily cycle is exhausted. At the end of a day, the state of the system is compared with that at the beginning of the day. If the states (temperature profile in the wall and room air temperature) agree to within a specified small tolerance, the solution has converged. If not, the daily cycle is repeated with new initial conditions equal to the present state of the system. Note that whenever the auxiliary energy source switches, new t^*(cumulative time, i.e.: $t_1 + t_2 + t_3 + \cdots$) should be used for the weather equations, (15) and (16).

After obtaining all times for switchover points, a graph of T_A versus time for a 24 hour period is processed, and inspected for consistency. In the case of heating, T_A is not supposed to be below (−DB) in Fig. 1. T_A below (−DB) means that the switchover point is missed, and the times are recalculated after readjusting the input data points for the bisection method.

Total heating or cooling time per day is obtained by summing the times during which the auxiliary energy is on. Then, heating/cooling loads per day can be calculated.

Formal calculation of cycle rate can be obtained as follows:

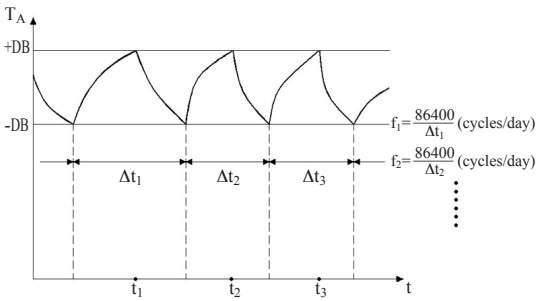

Fig. 2. Calculation method for cycle frequency.

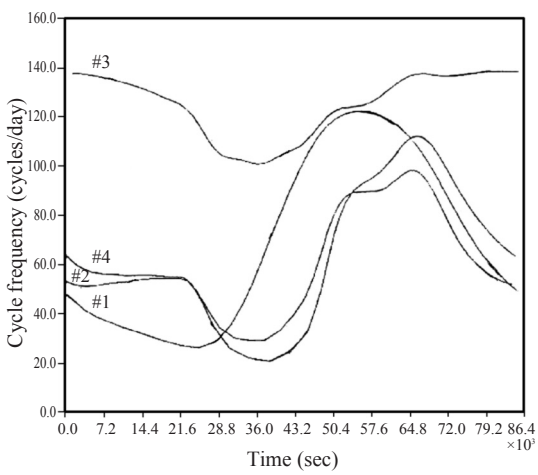

Fig. 3. Cycle frequency vs. time (Miami, August).

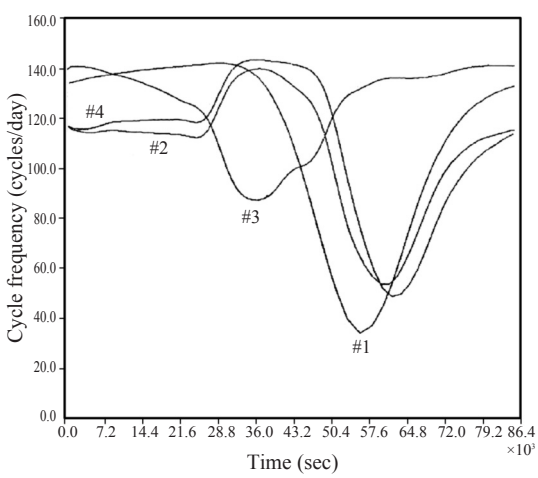

Fig. 4. Cycle frequency vs. time (Washington D.C., January).

$$f_n = 86400/(\Delta t_n) \quad (17)$$

where f_n is the cycle frequency (cycles/day) and Δt_n is the time interval for one cycle (secs/cycle) as shown in Fig. 2. Results for all four houses are shown in Fig. 3 for Miami (cooling) and Fig. 4 for Washington D.C. (heating). Frequent cycling exists in August in Miami for house #3. House #3 also shows the lowest variation in cycle rate compared with the other insulated houses. House #1 shows the highest variation in cycle rate.

Simplified technique

Two models are presented to approximate the energy consumption load and to investigate the cycling rate. Zero capacitance model is used for calculating the energy consumption approximately and simplified dynamic model is used for investigating the cycling rate.

The detailed results using accurate analytical solution require a large number of complex and repetitive calculations. Coding a computer program and using it is time-consuming and a boring job. It is desirable, therefore, for the engineer or building designer to have a method to quickly estimate the energy load for buildings .

A steady-state analysis is introduced to approximate the load. As shown in Fig. 5, ambient temperature and solar radiation can be combined in the form of the sol-air temperature in ASHRAE handbook (1982) to simplify the analysis. The sol-air temperature is that outdoor air temperature which, in the absence of all radiative exchange, gives the same rate of heat input to the surface of the wall as exists with the actual incident solar radiation, radiant energy exchange with the sky and other outdoor surroundings, and convective heat

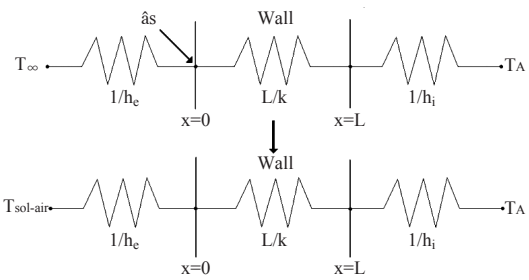

Fig. 5. Sol-air temperature for steady-state analysis.

exchange with the outdoor air. It is represented as follows:

$$T_{sol-air} + T_\infty + \hat{a}S/h_e - \varepsilon \Delta R/h_e \tag{18}$$

where ε is hemispherical emittance of the surface, and ΔR is the difference between the long wave radiation incident on the surface from the sky and surroundings, and the radiation emitted by a blackbody at ambient temperature.

It is difficult to determine an accurate value of ΔR, since vertical surfaces receive long wave radiation from the ground and surrounding buildings as well as from the sky. When the solar radiation intensity is high, surfaces of terrestrial objects usually have a higher temperature than the ambient air temperature; thus, their long wave radiation compensates to some extent for the sky′s low emittance. Also, during the day, the solar exchange typically dwarfs the long wave radiative exchange. Therefore, it is reasonable to assume $\Delta R = 0$ for vertical surfaces. Equation (18) can then be rewritten as:

$$T_{sol-air} = T_\infty + \hat{a}S/h_e \tag{19}$$

Thus, the steady-state heat flow for the building maybe calculated as:

$$Q_S = \pm UA\,(\overline{T_{sol-air}} - T^*_A) + C_A{}'I\,(\overline{T_\infty} - T^*_A)$$
(+ sign: cooling, − sign: heating) (20)

$$U = 1/(1/h_e + L/k + 1/h_i) \tag{21}$$

where U is overall heat transfer coefficient, $\overline{T_{sol-air}}$, $\overline{T_\infty}$ and T^*_A are the average sol-air temperature, ambient temperature and room air temperature, respectively.

Here, heat flow by infiltration is added to Q in equation (20). Two average room air temperatures are used for T^*_A: one is the set-point temperature T_s, which is 22, and the other is the average room air temperature from the computer output in the case of the on-off controller, $\overline{T_A}$.

The study now turns its attention to the simplified dynamic model for investigating the cycling rate. In this model, T_L is assumed to be known, and equation (5).

Equation (5) is rearranged as follows:

$$dT_A/dt + (a^* + b^*)T_A = a^*T_L + b^*T_\infty + c^* \tag{22}$$

where:

$$a^* = h_i A/C_A \tag{23}$$

$$b^* = C_A{}'I/C_A \tag{24}$$

$$c^* = Q/C_A \tag{25}$$

Equation (22) becomes:

$$dT_A/dt + B^*T_A = A^* \tag{26}$$

when:

$$A^* = a^*T_L + b^*T_\infty + c^* \tag{27}$$

$$B^* = a^* + b^* \tag{28}$$

A^* is assumed constant, as T_L and T_∞ are nearly constant for a short cycle period.

Equation (26) is solved subject to initial conditions over the cycle interval. There are two initial conditions to be considered: one is the room air temperature, T_A, at the upper bound of the

deadband, the other is T_A at the lower bound of the deadband. For convenience, let T_A at the upper bound be T_A^+, and T_A at the lower bound be T_A^-, respectively. c^* becomes Q/C_A or zero, depending on whether the auxiliary energy source is on or off.

Solutions to equation (26) for the heating case are shown below:

1) For heating cycle,

$$T_A = (T_A^- - A^*/B^*)\ \mathrm{EXP}\ (-B^*t) + A^*/B^* \qquad (29)$$

2) For no-heating cycle,

$$T_A = (T_A^+ - A^*/B^*)\ \mathrm{EXP}\ (-B^*t) + A^*/B^* \qquad (30)$$

No-heating cycle implies that the room air temperature variation in the case of no auxiliary energy (Q=0). Solutions to equation (26) for the cooling case are reversed.

Table 2. Average temperatures and energy consumption loads for steady-state ($T_A = T_s$)

City, Month, House #	$\overline{T_{sol\text{-}air}}$	$\overline{T_0}$	$\overline{T_L}$	Energy consumption load (MJ/day)
AA1	30.20	29.95	22.42	4.367
AA2	29.80	29.59	22.36	3.756
AA3	29.80	29.25	22.94	9.520
AA4	29.50	29.28	22.38	3.920
AJ1	9.84	10.21	21.37	7.502
AJ2	9.30	9.64	21.41	7.189
AJ3	9.30	10.19	20.47	16.144
AJ4	8.89	9.28	21.33	7.635
MA1	32.00	31.70	22.52	5.528
MA2	31.74	31.48	22.45	4.902
MA3	31.74	31.05	23.17	12.015
MA4	31.54	31.26	22.48	5.141
MJ1	26.07	25.95	22.21	1.992
MJ2	25.68	25.58	22.17	1.589
MJ3	25.68	25.42	22.44	4.381
MJ4	25.38	25.28	22.17	1.633
SA1	21.71	21.72	21.99	0.502
SA2	21.34	21.36	21.97	0.681
SA3	21.34	21.39	21.92	1.024
SA4	21.07	21.10	21.95	0.751
SJ1	16.05	16.23	21.69	3.818
SJ2	15.62	15.79	21.70	3.751
SJ3	15.62	16.07	21.23	8.194
SJ4	15.30	15.50	21.66	3.998
WA1	28.69	28.49	22.34	3.556
WA2	28.36	28.19	22.29	3.055
WA3	28.36	27.91	22.77	7.758
WA4	28.11	27.93	22.31	3.188
WJ1	4.64	5.16	21.10	10.322
WJ2	4.30	4.78	21.18	9.649
WJ3	4.30	5.55	19.87	22.278
WJ4	4.04	5.57	21.09	10.209

Equations (29) and (30) are rearranged to yield the partial cycle time t as:

$$t=(1/B^*)\ln[(T_A^- - A^*/B^*)/(T_A - A^*/B^*)] \quad (31)$$

$$t=(1/B^*)\ln[(T_A^+ - A^*/B^*)/(T_A - A^*/B^*)] \quad (32)$$

Cycling times are calculated by using equations (31) and (32), and these results are compared with actual computer results from the exact solution.

Results and discussion

Two average room air temperatures are used for T_A^*: one is the set-point temperature T_s, which is 22CENTIGRADE, and the other is the average room air temperature from the computer output in the case of the on-off controller, $\overline{T_A}$.

Results for the former case are given in Table 2 and for the latter case in Table 3. Average ambient temperature ($\overline{T_\infty}$) and average solar flux ($\overline{S}$) from the DC components b_0, and d_0, respectively, are used.

Energy consumption loads resulting from the steady-state analysis are compared in Table 4 with those from the numerical solution for on-off control. The approximate results using a steady-state analysis are, in most cases, in close agreement with the exact results for the case of a on-off controller. The reason for large error is that the steady-state analysis does not include thermal mass effects. Therefore, the exact results of energy load for houses #2 and #4 in mild weather areas are very different from those of the steady-state analysis. However, the error is very small in locations where the temperature difference between the average sol-air temperature and the set-point temperature is high, Thus, the steady-state method is fairly accurate when estimating energy loads in extreme weather conditions.

The steady-state method represents a reasonable compromise between accuracy and ease of application, even though more accurate computer models can simulate actual weather conditions and buildings.

Table 3. Energy consumption loads (T_A^* from computer output for an on-off controller case)

City, Month, House #	Energy consumption load (MJ/day)	City, Month, House #	Energy consumption load (MJ/day)
AA1	4.865	SA1	1.528
AA2	3.493	SA2	0.239
AA3	9.195	SA3	0.622
AA4	3.647	SA4	0.273
AJ1	7.569	SJ1	4.355
AJ2	7.034	SJ2	3.515
AJ3	16.110	SJ3	7.762
AJ4	7.472	SJ4	3.746
MA1	5.365	WA1	3.520
MA2	4.678	WA2	2.766
MA3	11.844	WA3	7.311
MA4	4.901	WA4	2.878
MJ1	2.262	WJ1	10.242
MJ2	1.235	WJ2	9.544
MJ3	3.782	WJ3	22.449
MJ4	1.213	WJ4	10.099

Table 4. Load comparison

City, Month, House #	Calculated load with on-off controller (MJ/day)	Approximated load (MJ/day)	% Error
AA1	4.210	4.865	13.5
AA2	3.576	3.493	2.4
AA3	9.011	9.195	2.0
AA4	4.022	3.647	10.3
AJ1	7.496	7.569	1.0
AJ2	7.384	7.034	5.0
AJ3	16.110	16.110	0.0
AJ4	8.002	7.472	7.1
MA1	5.246	5.365	2.2
MA2	4.534	4.678	3.1
MA3	11.739	11.844	0.9
MA4	4.965	4.901	1.3
MJ1	2.203	2.262	2.6
MJ2	1.498	1.235	21.3
MJ3	3.433	3.782	9.2
MJ4	0.361	1.213	70.2
SA1	1.463	1.528	4.3
SA2	0.068	0.239	71.6
SA3	0.519	0.622	16.6
SA4	0.143	0.273	47.6
SJ1	4.248	4.355	2.5
SJ2	4.125	3.515	17.4
SJ3	7.555	7.762	2.7
SJ4	4.755	3.746	26.9
WA1	3.455	3.520	1.9
WA2	2.797	2.766	1.1
WA3	6.997	7.311	4.3
WA4	3.132	2.878	8.8
WJ1	10.092	10.242	1.5
WJ2	9.521	9.544	0.2
WJ3	22.564	22.449	0.5
WJ4	10.188	10.099	0.9

Five types of results in simplified dynamic model are presented: (1) exact results, (2) results obtained using the average of T_L at the start of the cycle, T_L at the end of the cycle from the exact solution, and using T_0 at the beginning of the cycle, (3) results obtained using T_L and T_∞ at the beginning of the cycle, (4) results obtained using time averaged values of T_L and T_∞ from the exact solution, and (5) results obtained using averaged values of T_L and T_∞ from the steady-state analysis.

Results are calculated in two groups. Group I is in the low cycling region and group II is in the high cycling region. Cycle times for energy on and energy off (i.e. partial cycle times) are calculated,

and presented in Tables 5 and 6 for groups I and II, respectively. Results are presented in five columns, for types one through five as mentioned above. Two results are presented in each column. The first result, preceding the comma, is for increasing T_A (heating in January, no cooling in August). The second result, after the comma, is for decreasing T_A (no heating in January, cooling in August). A hyphen (−) is used in both Tables to indicate an unobtainable result.

As shown in the Tables, cycle time cannot be obtained in many cases when the exact cycle time is long. Also, cycle time is very sensitive to the value of , The approximate results for "type two" in the Tables are very close to the exact values where they are obtainable. The maximum error is less than 5%, and most have an error of less than 2%. However, the error is seen to increase when average values of and from the exact solution or from the steady-state analysis are used.

In the case of Santa Maria in August, using two groups is not possible due to the very low cycling rate. Houses #2 and #4 are not modelled due to extremely low cycling rate. It is concluded that the simple dynamic model is applicable for high cycling rates only, and and (i.e. the "type two" in Tables 5 and 6) must be chosen very carefully to obtain useful answers.

Conclusions

An analytical solution based on a rigorous mathematical model has proved effective in

Table 5. Comparison of cycling time in seconds (on-off controller, simple dynamic model, group I)

City, Month, House #	Result type				
	1	2	3	4	5
MA1	265, 165	-, 166	-, 199	-, 177	-, 161
MA2	2357, 180	-, 180	-, 198	-, 183	-, 157
MA3	622, 207	626, 206	911, 216	453, 226	544, 213
MA4	3171, 181	-, 181	-, 196	-, 187	-, 158
SA1	170, 1468	171, -	204, -	89, -	135, -
SA3	185, 2401	185, -	196, -	150, -	137, -
WJ1	167, 2382	167, -	200, -	206, 625	197, 963
WJ2	185, 1424	185, -	202, -	208, 597	190, -
WJ3	395, 246	390, 242	431, 254	439, 229	511, 216
WJ4	186, 1591	186, -	200, -	215, 522	195, 1190

Table 6. Comparison of cycling time in seconds (on-off controller, simple dynamic model, group II)

City, Month, House #	Result type				
	1	2	3	4	5
MA1	495, 213	551, 212	-, 263	-, 177	-, 161
MA2	770, 200	925, 197	-, 211	453, 183	-, 157
MA3	442, 233	436, 230	497, 241	-, 226	544, 213
MA4	698, 204	743, 201	-, 213	-, 187	-, 158
WJ1	256, 353	254, 358	333, 609	206, 625	197, 963
WJ2	227, 469	223, 458	240, 606	208, 597	190, -
WJ3	585, 209	579, 208	736, 219	439, 229	511, 216
WJ4	231, 443	228, 441	243, 527	215, 522	195, 1190

comparing the energy consumption in four different types of houses and weather conditions. Such a solution may not be applicable to situations involving layers of highly (thermally) dissimilar materials. However, by virtue of the novel approach of derivation of appropriate effective properties, the method should be extendable somewhat beyond the case of a purely homogeneous material.

A clearer understanding of the limitations and the capabilities of two simplified techniques, a steady-state analysis and a dynamic model, were obtained.

The steady-state analysis gives an accurate estimate of energy load for all types of construction when there exists large differences between set-point temperature and average sol-air temperature. Thus, the steady-state method is fairly accurate when estimating energy loads in extreme weather conditions. The steady-state method represents a reasonable compromise between accuracy and ease of application.

There is, in all types of construction, significant coupling between the structure, the weather conditions, and the cycling rate. Only in extreme cases when there was negligible penetration of the thermal wave to the interior of the building was it possible to obtain good agreement between the calculated cycling rate and that predicted from the simplified model.

A limiting criterion should be developed for when the steady-state model begins to provide inaccurate results. Presumably, this would involve some number of the non-dimensional terms.

Should this limiting criterion be developed, a correction factor to the energy use predicted by the steady-state model should be developed. This can take the form of an empirical curve fit versus the applicable non-dimensional parameters.

References

ASHRAE handbook of 1981 fundamentals, 1982. American Society of Heating, Refrigerating and Air-Conditioning Engineers, Inc., 21.1－21.9.

Brigham, E.O., 2004. The fast Fourier transform. Prentice Hall, Inc., 25－150.

Burch, D. M., D.F. Kritz and R.S. Spain, 1984. The effect of wall mass on winter heating loads and indoor comfort-an experimental study. ASHRAE Transactions 90, Part 1, 94－l21.

Burch, D.M., S.A. Malcolm and K.L. Davis, 1984. The effect of wall mass on the summer space cooling of six test buildings. ASHRAE Transactions 90, Part 1, 5－20.

Carslaw, H.S. and J.C. Jaeger, 1959. Conduction of heat in solids. Oxford Press, Great Britain, 92－326.

Cuplinskas, E.L., 1977. Thermal response calculations by the finite differences method. ASHRAE Transactions 83, Part 2, 118－131.

Jones, R.F. and G. Dennehy, 1982. The mastin double-envelope house: a thermal performance evaluation. Passive Solar Journal, 1 (3), 151－174.

Kreyszig, E., 2006. Advanced engineering mathematics. John Wiley & Sons, Inc, 220－270.

Kusuda, T., 1976. Procedure employed by the ASHRAE task group for the determination of heating and cooling loads for building energy analysis. ASHRAE Transactions 82, Part 1, 305－314.

Kusuda, T., 1981. A comparison of energy calculation procedures. ASHRAE Journal, Vol. 23, 21－24.

Mitalas, G.P. and D.G. Stephenson, 1967. Room thermal response factors. ASHRAE Transactions 73, Part 1, III.2.1－III.2.10.

Mitalas, G.P., 1968. Calculation of transient heat flow through walls and roofs. ASHRAE Transactions 74, Part 2, 182－188.

Myers, G.E., 2001. Analytical methods in conduction heat transfer. McGraW-Hill, Inc., New York, 175－205.

Peavy, B.A., F.J. Powell and D.M. Burch, 1973. Dynamic thermal performance of an experimental masonry

building. U.S. National Bureau of Standards, Building Science Series 45, 112－136.

Stephenson, D.G. and G.P. Mitalas, 1967. Cooling load calculations by thermal response factor method. ASHRAE Transactions 73, Part 1, III.1.1－III.1.7.

Tape Deck #9734, 1998. Typical meteorological year (TMY). Sandia Report, 7－120.

Webster, D.W., 1985. Variable-base degree-days and the analysis of energy performance for small buildings. ASHRAE Transactions 91, Part 1B, 907－915.

2010년 12월 14일 접수
2011년 1월 26일 수정
2011년 1월 28일 수리